Mechanical properties of zirconia-coated 316L austenitic stainless steel

M. ATIK, S. H. MESSADDEQ, M. A. AEGERTER
Departamento de Física e Ciência dos Materiais, Instituto de Física de São Carlos, Universidade de São Paulo, C. P. 369 - 13560-970 - São Carlos - SP - Brazil

J. ZARZYCKI
Laboratoire de Science des Matériaux Vitreux, Université de Montpellier II, 134095 Montpellier Cedex 5, France

Zirconia is a material known for its excellent physico-chemical properties, such as mechanical strength, ionic conductivity, heat resistance against oxidation and chemical durability (alkali resistance). Its use for coating on steels in order to improve the surface against environment attack is one of the most promising applications [1–6]. The mechanical properties, such as microhardness, Young's modulus and fracture toughness of these films are also important parameters to characterize the abrasion resistance, cutting, machining or scratching of these materials [7–11]. Vickers microhardness testing provides a simple and efficient means for evaluating and determining the performance and reliability of such coatings.

In this letter we report on sol–gel zirconia films prepared from sonocatalysed sols deposited by a dip-coating technique on 316L austenitic stainless steel in order to increase the substrate surface hardness. The mechanical properties of crystalline zirconia film (0.75 μm thick) have been investigated using an indentation technique as a function of the load and indentation depth. The data are analysed using Meyer's equation [12] and the Jönnson and Hogmark model [13].

The solutions were prepared by dissolving zirconium propoxide $Zr(OC_3H_7)_4$ in isopropanol (C_3H_7OH) with a small amount of glacial acetic acid (CH_3COOH) and excess of water, using an ultrasound irradiation technique (Sonicator Heat Systems Ultrasonics W385, 20 kHz). The volume ratios H_2O/C_3H_7OH and H_2O/CH_3COOH were equal to 1 and 2, respectively, and the concentration of the starting alkoxide solutions was varied between 0.2 and 0.9 mol/l ZrO_2. The resulting sols are clear, transparent and can be kept for 4 weeks at room temperature without gelification.

The 316L stainless steel substrates used in this study have the nominal composition (wt%): 67.25 Fe, 18.55 Cr, 11.16 Ni, 2.01 Mo, 0.026 Cu, 0.15 Si and 0.028 C. Samples (30 mm × 20 mm × 0.4 mm) were mechanically cut from large foils, degreased ultrasonically in acetone and then cleaned with distilled water. Single-layer coatings have been deposited by a dip-coating process, withdrawing the substrates from the solution at a constant rate of 10 cm/min. The gel films were dried at 60 °C for 15 min and then densified in a furnace in air atmosphere, increasing the temperature at a rate of 5 °C/min with two isothermal holdings, first at 450 °C for 1 h and then at 800 °C for 2 h. The resulting coatings have a thickness (measured by ellipsometry) which varied between 0.35 and 0.8 μm, depending on the sol concentration [6]. In the work reported here, 0.75 μm thick coatings were used.

X-ray diffraction patterns of the coatings were recorded with a Rigaku Rotaflex diffractometer with a CuK_α irradiation of (0.15418 nm). A Bomen FTIR was used to obtain high resolution optical reflection spectra of the coatings in the range 400–4000 cm^{-1} at an incident angle of 30°. The ZrO_2 surface was observed by scanning electron microscopy (Zeiss 960). Vickers microhardness tests (H_v) were realized with a Carl Zeiss 160 Microhardness Tester using loads of 5 to 200 g by measuring the diagonals of the pyramidal diamond indenter of at least six indentations for each load. The load was applied for 16 s. The two indentation diagonals d_1, d_2 determined for each indentation were averaged to yield $D = 0.5\ (d_1 + d_2)$. The H_v obtained from the ratio of the applied load to the resulting indented area is expressed as [14]:

$$H_v = 1854.4P/D^2 \qquad (kg/mm^2) \qquad (1)$$

where P(g) is the applied load on the indenter and D (μm) is the average of both diagonals of the indentation. The Vickers indentation depth is $h = D/7$ [15].

X-ray diffraction data of the uncoated and coated substrates are shown in Fig. 1. As-received stainless steel shows three distinct peaks with d values equal to 0.208, 0.180 and 0.127 nm which correspond to the Cr + Fe + Ni cubic phase (Fig. 1a). After heat treatment at 800 °C for 2 h in air, the first peak decreases in intensity and other peaks appear with $d = 0.364$, 0.267 and 0.25 nm, corresponding to the formation of cubic and hexagonal Cr_2O_3 (Fig. 1b). Substrates coated with ZrO_2 film and heat-treated at 800 °C for 2 h show the same peaks seen in Fig. 1a and one additional peak at 0.298 nm, corresponding to crystalline tetragonal zirconia (Fig. 1c). There is no change in relative intensity of the cubic metal peaks, indicating that no observable oxidation has occurred at the metal/film interface during the heat treatment.

The infrared reflection spectra of the coatings deposited on stainless steel is given in Fig. 2. At

0261-8028

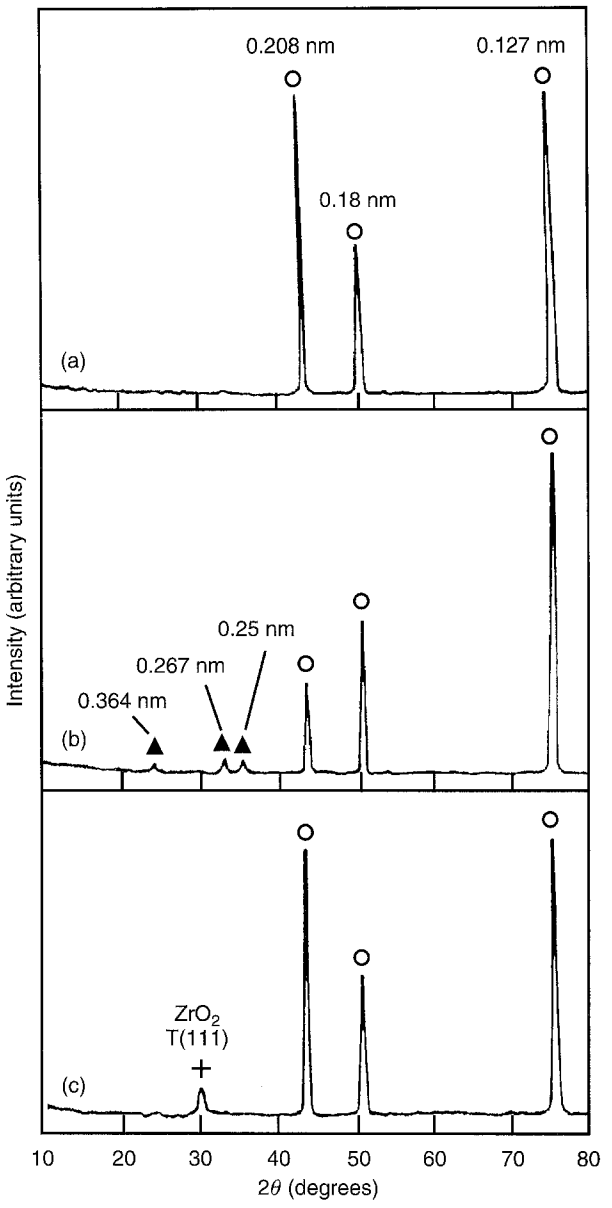

Figure 1 X-ray diffraction of austenitic stainless steel: (a) as-received (uncoated); (b) uncoated but oxidized in air at 800 °C for 2 h; (c) ZrO_2-coated after oxidation at 800 °C for 2 h.

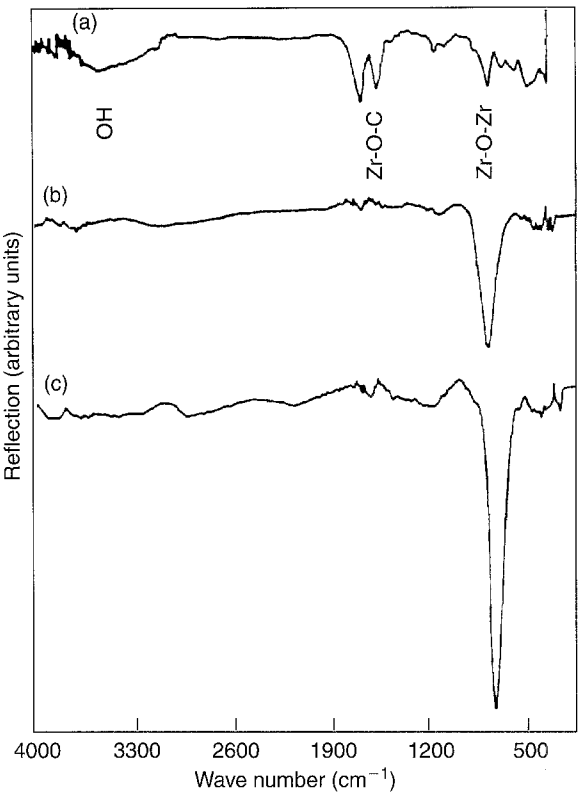

Figure 2 IR reflection spectra of ZrO_2 films deposited on stainless steel: (a) after deposition at room temperature; (b) after densification at 450 °C for 1 h; (c) after densification in air at 800 °C for 2 h.

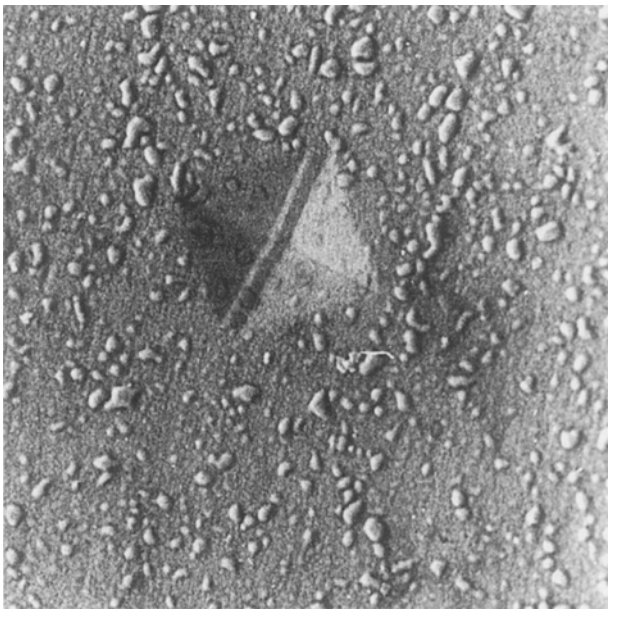

Figure 3 Vickers indentation on the surface of a zirconia coating showing a perfect pyramid form.

room temperature (Fig. 2a), the absorption due to OH groups is observed near 3200–3600 cm^{-1} and the bands observed at 1452–1578 cm^{-1} are characteristics of Zr–O–C species. Absorption bands due to Zr–O–Zr species are observed near 666 and 363 cm^{-1} [6]. The evolution of the spectra with thermal treatment of the samples shows that the Zr–O–C absorption decreases and eventually disappears while that of Zr–O–Zr increases strongly with firing time and temperature (Figs 2b–c).

Fig. 3 shows a typical micrograph of an indentation performed on the surface of substrate coated with 0.75 μm thick zirconia film after heating at 800 °C in air for 2 h. In most cases the indentations showed a perfect pyramidal form without visible cracks appearing around the indentations.

Fig. 4 shows a typical load–penetration depth curve for indentation of 0.75 μm zirconia coating on 316L austenitic stainless steel substrate heat-treated at 800 °C for 2 h in air. The indentation depth increases with increasing applied load and the initial variation of the loading curve is approximately parabolic. The variation of the microhardness values, calculated by Equation 1, as a function of the applied load, is shown in Fig. 5. The hardness of the film/substrate system decreases from 760 kg mm^{-2} measured for a 5 g load to about 300 kg mm^{-2} for a 50 g load and then becomes constant for larger loads (Fig. 5a), while the hardness of the uncoated substrate heat-treated at 800 °C for 2 h in air (same conditions) remains constant at around 300 kg mm^{-2} in the same load range (Fig. 5b).

Usually the hardness should be independent of the size of the indent. A variation as a function of the

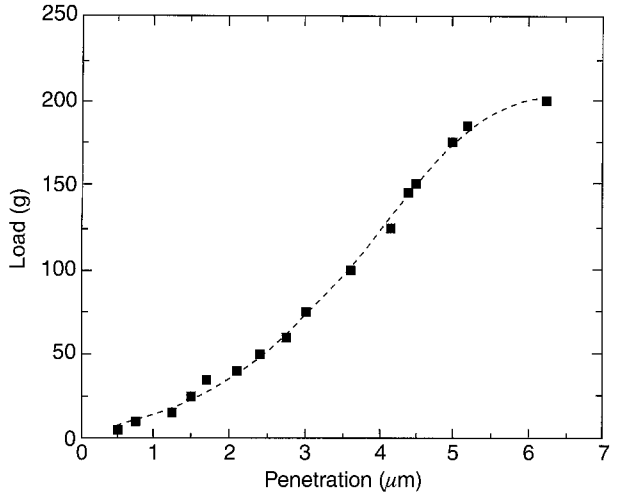

Figure 4 Load–penetration curve obtained by indentation of 0.75 μm thick ZrO_2 films deposited on 316L stainless steel sintered to 800 °C for 2 h (the lines drawn are for eye guidance only).

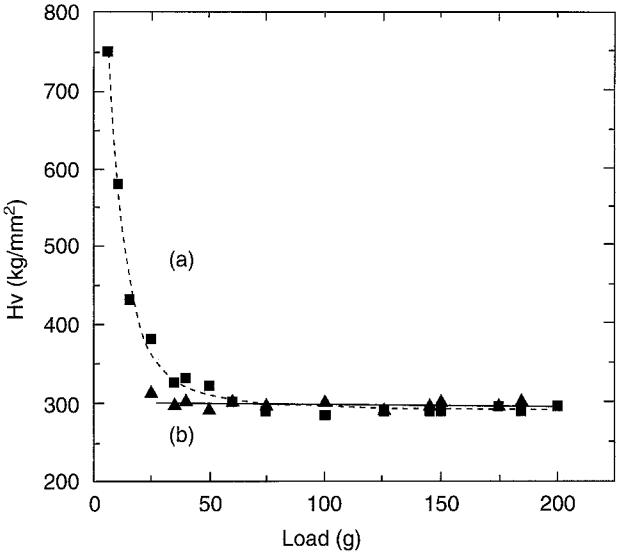

Figure 5 Vickers hardness versus load for (■) ZrO_2 coated stainless steel after heat treatment at 800 °C for 2 h; (▲) uncoated stainless steel but heat treated at 800 °C for 2 h.

load as observed for the film/substrate system indicates a significant indentation size effect (ISE). This phenomenon can be modelled by a power law known as Meyer's equation [12]:

$$P = kD^n \tag{2}$$

where k is a constant and n is a constant, called the Meyer index and used as a measure of ISE. When the hardness is independent of the load, $n = 2$. If the hardness increases with the applied load, $n > 2$ and if the hardness decreases with the applied load, $n < 2$.

For the film/substrate system the hardness decreases with the applied load up to ~75 g indicating that $n \leqslant 2$ and then becomes independent for larger values indicating that $n \approx 2$. The determination of n can be done by measuring the slope of the curve in a plot of $\log P$ versus $\log D$ or $\log h$. However Yurkov *et al.* [15] have suggested another approach which provides the coefficient n at any point of the curve:

$$n = [\log(H_1/H_2)/\log(h_1/h_2)] + 2 \tag{3}$$

Such a plot is shown in Fig. 6 for both systems. For the heat-treated substrate, the values of n are constant and equal to ~2 (Fig. 6a). For the film/substrate system $n \approx 1.35$ down to a depth of 1.5 μm (twice the film thickness) indicating a strong ISE (Fig. 6b), but no such effect is observed with the heat-treated bare substrate. A thorough description of this effect needs more data in the depth range 0–1.5 μm which, unfortunately, could not be registered with our equipment as no indent could be observed for loads smaller than 5 g. As the depth of indent increases, n increases monotonically (transition region) to reach eventually steady values slightly above 2 for $t > 3.5$ μm, where no ISE is expected.

The data were also fitted to the model proposed by Jönnson and Hogmark [13] which combines the hardness of the film and substrate via a geometrical approach. In this model the composite hardness is determined by the weighted average of the film and substrate hardnesses in proportion to the deformed areas (Fig. 7). The film is considered to provide support only at the margin of the indentation area and elsewhere is assumed to be broken by the indent transmitting the load directly onto the substrate. The model does not take into account the indentation size effect and is only valid for indentation depth larger than the thickness of the film t, in our case 0.75 μm. The composite Vickers hardness is given by:

$$H_c = (A_f/A)H_f + (A_s/A)H_s \tag{4}$$

where A_f and A_s are the geometrical supporting areas, $A = A_f + A_s$ is the total projected area of the imprint which is left on the indented surface, and H_f and H_s are the hardness of the film and substrate, respectively. A simple geometrical analysis leads to:

$$H_c = H_s + [(2Ct/h) - C^2(t/h)^2](H_f - H_s) \tag{5}$$

where $C = 2\sin^2 11° = 0.073$ if $H_f \gg H_s$, or $C = \sin^2 22° = 0.14$ if $H_f \approx H_s$, and φ is the angle between the tip sides with the coating surface

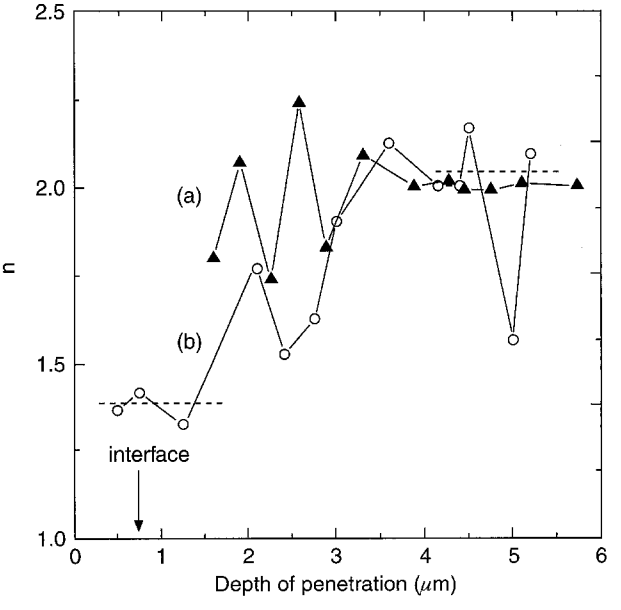

Figure 6 Values of Meyer's index n, versus penetration of the indentor for ZrO_2 film 0.75 μm thick deposited on SS (○) and bare substrate (▲) both heat treated at 800 °C for 2 h.

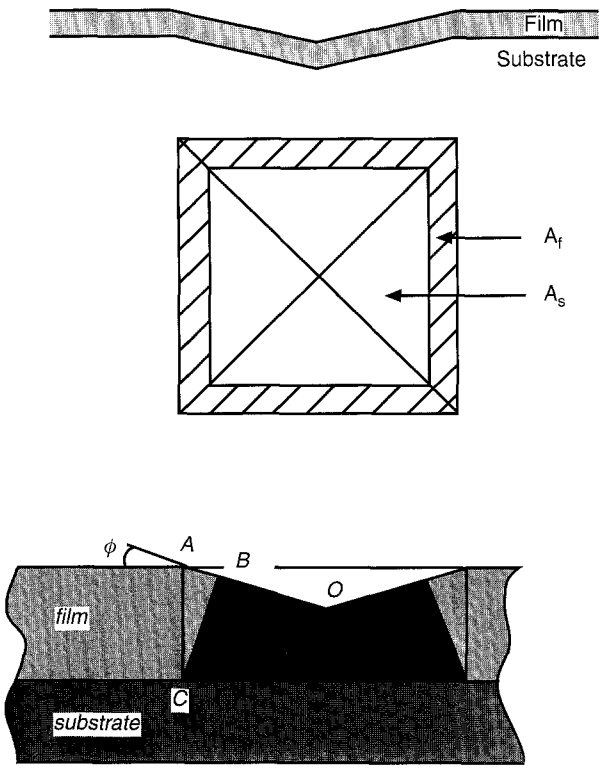

Figure 7 Geometry of indentation (for pyramidal indenter) to determine the composite hardness proposed by Jönnson and Hogmark [13]. The load is applied to the films within the area A_f and to the substrate within A_s.

($\varphi = 22°$ for a Vickers indentation). Since φ is determined by the geometry of the indentation tip, the only free choice of parameters are C, H_f and H_s.

As the ratio of the indentation depth h to film thickness t is larger than 1 at all applied loads larger than 10 g (Fig. 4), this model is applicable for almost all experimental data. As shown in Fig. 5, the hardness of the film H_f measured at the lowest load (760 kg mm^{-2}) is higher than the hardness of the substrate H_s (300 kg mm^{-2}). Fig. 8 shows that experimental data can be also satisfactorily fitted with this model using the values $C = 0.073$, $H_f = 760$ kg mm^{-2} and $H_s = 300$ kg mm^{-2}. Usually it is admitted that the true hardness of a film should be measured using penetration depth not larger than one fifth of the film thickness (in our case 0.15 μm). Therefore the chosen value $H_f = 760$ kg mm^{-2} corresponds to apparent hardness and the true value should be higher.

These two models apparently fit the experimental data. At the present stage of knowledge, it is, however, not possible to choose which one better describes the physical behaviour of the coatings.

The letter reports on the preparation of zirconia films dip-coated on 316L austenitic stainless steel substrate, the sol being made with a sonocatalytic method. Single coatings densified at 800 °C in air for 2 h have a thickness of about 0.75 μm and are crystalline with a tetragonal structure. Microhardness of these materials showed a significant increase from 300 to 760 kg mm^{-2} indicating that the zirconia

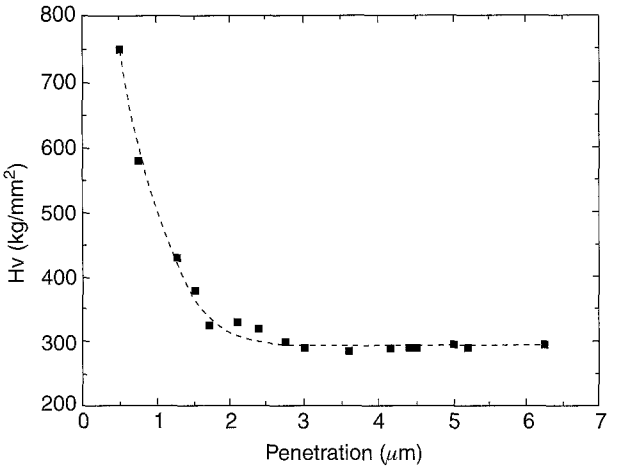

Figure 8 Composite hardness versus penetration depth of 0.75 μm thick ZrO_2 films deposited on 316L stainless steel sintered to 800 °C for 2 h.

coatings improve the mechanical resistance of the stainless steel substrates. The hardness of the coating decreases with the load applied on the indent. This phenomenon is due to the effects of indentation size and substrate hardness. Both models describe the effects of film/substrate deformations and the method is applicable provided the h/t ratio is larger than 1.

References

1. A. H. HEVER and L. W. HOBBS, "Advances in ceramics", Vol. 3 (American Ceramic Society, Columbus OH, 1981).
2. M. ATIK and M. A. AEGERTER, *J. Non-Cryst. Solids* **147&148** (1992) 818.
3. K. SUGIOKA, H. TASHIRO, K. TOYODA, H. MURAKAMI and H. TAKAI, *J. Mater. Res.* **5** (1990) 2835.
4. P. LIMA NETO, M. ATIK, L. AVACA and M. A. AEGERTER, *J. Sol–Gel Technol.* **1** (1994) 177.
5. K. IZUMI, M. MURAKAMI, T. DEGUCHI and A. MORITA, *J. Amer. Ceram. Soc.* **72** (1989) 1465.
6. M. ATIK, C. R'KHA and J. ZARZYCKI, *J. Mater. Sci. Lett.* **13** (1994) 266.
7. A. G. EVANS and E. A. CHARLES, *J. Amer. Ceram. Soc.* **59** (1976) 371.
8. B. R. LAWN, A. G. EVANS and D. B. MARSHALL, *ibid.* **63** (1980) 574.
9. P. MIRAZONO and J. S. MOYA, *Ceram. Int.* **10** (1984) 147.
10. D. T. QUINTO, G. J. WOLFE and P. C. JINDAL, *Thin Solid Films* **153** (1987) 19.
11. K. WASA, T. NAGAI and S. HAYAKAWA, *ibid.* **30** (1975) 235.
12. I. J. McCOLM, "Ceramic hardness" (Plenum, New York, 1990).
13. B. JÖNNSON and S. HOGMARK, *Thin Solid Films* **144** (1984) 257.
14. Y. H. CHRIS CHA, G. KIM, H. J. DOERR and R. F. BUNSHAH, *ibid.* **253** (1994) 212.
15. A. L. YURKOV, N. V. JHURAVLEVA and E. S. LUKIN, *J. Mater. Sci.* **29** (1994) 6551.